 Transactions on Modelling and Simulation vol 10, © 1995 WIT Press, www.witpress.com, ISSN 1743-355X

Heat transfer to a bubble in a liquid layer near a solid plate in a finite cell

L. Huang, D. Rumschitzki, Z. Dagan
Department of Mechanical Engineering, The City College of the City University of New York, New York, NY 10031, USA

Abstract

Incipient nucleate pool boiling and strong bubble-bubble interactions feature dramatic heat transfer enhancements associated with liquid vaporization. We employ numerical methods to show that very high heat transfer towards the bubble-heating surface contact line is the likely mechanism in the former case. To study these phenomena, we employ a boundary element method together with an asymptotic expansion of the contact line region in order to determine the quasistatic temperature field around a spherical vapor bubble on or near a solid-liquid interface in a periodic cell. Both the heating solid and the liquid layer are of finite depth perpendicular to their mutual interface and one may arbitrarily prescribe far field temperatures or heat fluxes. Narrow cell width calculations show heat transfer enchancement typical of bubble-bubble interactions.

1 Introduction

The problem of the growth rate of a bubble in pool boiling is of great importance in determining the overall heat transfer rate. So far only a few accurate theoretical solutions are known for the growth rate of a vapor bubble. Scriven [1] solved the bulk problem of a vapor bubble in a uniformly superheated homogenous liquid. Sadhal [2] offered analytical solutions to the problems of quasistatic heat transfer to a vapor bubble on or near a solid wall in an infinite domain with equal temperatures that exceed the saturation temperature far from the interface in both the solid and the liquid. Sadhal's solutions reveal a strong solid-liquid coupling in heterogeneous cases. However, with infinite domains his results cannot examine the interaction between bubbles, and with a superheated far field liquid they exclude the

majority of cases when heat derives solely from the wall. Both of these situations are of primary concern in the enhanced heat transfer rate during nucleate boiling. Huang and Dagan [3] used a collocation technique to get a semi-analytical solution for a vapor bubble suspended in a liquid near a solid-liquid interface in a semi-infinite layer. Their results demonstrated the effects of finite solid and liquid layer thicknesses on the imposed heat flux across the layers, and the solid-liquid coupling effect. However, their results offer no information on the interaction between the bubbles, or on the heat transfer enhancement that the bubbles attached to the solid surface arouse. These are the focuses of the present study.

Eddington and Kenning [4] first suggested that adjacent vapor bubbles on a heated surface could strongly interact. They found many more cavities on the surface that satisfied an appropriate activation criterion than were actually activated during boiling [5]. With high speed motion pictures, Judd and Lavadas [6] directly observed these interactions during nucleation. Chekanov [7] claimed that this interaction between adjacent sites could be either attractive, or repulsive. By using a gamma distribution analysis, Calka and Judd [8] showed that an active site will likely seed and activate inactive sites within its bubble departure radius. They also predicted that sites between one and three departure radii from the active site would experience inhibition while sites that are farther would feel no interaction at all. Although there is no commonly accepted explanation of this phenomenon, the consensus is that the nucleation sites do not act independently, but rather interact and influence each other's nucleation. The present investigation is a step towards understanding this influence.

2 General formulation

The present study examines the axisymmetric heat transfer to a spherical bubble of radius a, surrounded by a liquid layer of thickness H and thermal conductivity κ_ℓ. The bubble is attached to a solid plate of thickness h and thermal conductivity κ_s. The composite layers are bounded laterally by an insulated, reflecting, periodic, cylindrical boundary of radius R_c. This axisymmetric composite cell intends to model a uniformly distributed two dimensional bubble array on the solid plate. The coordinate system is cylindrical (R,Z,ψ) with origin at the center of the spherical bubble. The distance between the bubble center and the solid plate is d, and the contact angle, measured in the liquid between the solid-liquid interface and the liquid-vapor interface, is φ. Due to a strong surface tension, the bubble's interior pressure is higher than the surrounding liquid pressure and remains spherical (small capillary number). Thermodynamics dictates that its liquid-vapor interfacial temperature is always the corresponding saturation temperature T_v.

Heat transfer from the surrounding liquid causes bubble growth. An estimate for the growth time t_g is $a/\dot{a}$ (the dot denotes time differentiation),

while the viscous and diffusive time scales are $t_v \sim a^2/\nu_\ell$ and $t_d \sim a^2/\alpha_\ell$, respectively. Here, ν_ℓ denotes the liquid kinetic viscosity and α_ℓ its thermal diffusivity. For sufficiently small and slowly growing bubbles, the bubble's Reynolds number ($Re = a\dot{a}/\nu_\ell$) is small and the liquid's Prandtl number $Pr_\ell = \nu/\alpha$ is usually of order one. As a result, the bubble's growth time can far exceed the viscous time as well as its thermal diffusion time, namely, $t_v/t_g \cong Re \ll 1$ and $t_d/t_g \cong Re\, Pr_\ell \ll 1$. One can thus neglect the transient effects. Furthermore, for small Peclet number ($Pe = Re\, Pr_\ell$), the influence of convection in the liquid phase becomes insignificant, and heat transfers only by conduction. For the vapor phase, we consider the limiting case when the density, viscosity and thermal diffusivity are much smaller than those for the liquid so that the behavior of the vapor phase decouples from that of the liquid phase.

With these simplifications the governing equations for both liquid and solid phases reduce to Laplace equations. The temperature on the vapor surface stays at T_v; on the free surface of the liquid and on the solid surface far from the liquid we prescribe temperatures T_f, and T_s, respectively. On the lateral cell surface, the heat flux is zero, so as to satisfy the periodic conditions. At the solid-liquid interface, the temperature and the flux are both continuous. It is convenient to define the dimensionless temperature (primed) as $T'^{\ell,s} = (T^{\ell,s} - T_v)/(T_s - T_v)$, where the superscripts, ℓ and s, denote the liquid and solid phases respectively. The coordinates and lengths are in units of the spherical vapor bubble radius a and $\kappa = \kappa_\ell/\kappa_s$, respectively.

As in all boundary element calculations, the solutions are numerical using Green's theorem. Boundary nodes are constructed on the exterior surface of the solid and liquid layer, the cylindrical cell surface, the bubble surface and the solid-liquid interface. Once the numerical solution for the heat flux at each point on the bubble surface is known, one calculates the total heat supplied to the bubble in dimensional form by

$$Q = 2\pi\kappa_\ell a^2 \int_{-\pi/2+\varphi}^{\pi/2} \frac{\partial T^\ell}{\partial n} \sin(\tau)\, d\tau, \qquad (1)$$

where $\varphi=0$ when the bubble is tangent to or detached from the solid.

3 Numerical analysis in the contact region

For the cases of a bubble attached to a solid plate, both the geometric and physical boundary conditions become singular at the solid-liquid-vapor contact line. To avoid singularities, we construct a circular ring which intersects the vapor-liquid, liquid-solid, and solid-vapor interfaces at right angles close to the contact line. Very close to the contact line, the solution should be insensitive to the conditions in the liquid and solid far away from the interface. Thus, an asymptotic expansion of Sadhal's solution for the temperature gradient near the contact line can prescribe the normal flux on this circular ring, as long as the

cell size is large enough so that neighboring bubbles are not too close. Sadhal expresses his solution in terms of the toroidal coordinates (ξ,η,ψ), which are related to the cylindrical coordinates by the transformation,

$$Z = \frac{c \sin \eta}{\cosh \xi - \cos \eta} + c \cdot \mathrm{ctg}\, \varphi; \quad R = \frac{c \sinh \xi}{\cosh \xi - \cos \eta}. \tag{2}$$

Here, c is the radius of the contact line or the dry spot. In this coordinate system, the solid-liquid interface is $\eta=0$ and $0 \le \xi \le \infty$. The flux in the liquid and solid regions takes the form:

$$\frac{\partial T^{\ell,s}}{\partial n} = \frac{1}{M^2}\left[\left(\frac{\partial T^{\ell,s}}{\partial \xi}\frac{\partial R}{\partial \xi} + \frac{\partial T^{\ell,s}}{\partial \eta}\frac{\partial R}{\partial \eta}\right)e_R + \left(\frac{\partial T^{\ell,s}}{\partial \xi}\frac{\partial Z}{\partial \xi} + \frac{\partial T^{\ell,s}}{\partial \eta}\frac{\partial Z}{\partial \eta}\right)e_Z\right] \cdot \vec{n} \tag{3}$$

where $M=c/(\cos\xi - \cos\eta)$ is the metric parameter, $\vec{n}$ is the normal vector on the circular ring, and e_R and e_Z are the unit vectors in the R and Z directions, respectively. The partial derivatives of the temperatures in eqn (3) are as follows:

$$\partial T^s/\partial \eta = Be^{-\xi/2}(1-e^{-\xi\beta})\sqrt{2\cosh\xi - 2\cos\eta}$$
$$\{\cos((\eta+\pi)\beta)\sin\eta - 2\beta(\cosh\xi - \cos\eta)\sin((\eta+\pi)\beta)\} \tag{4}$$

$$\partial T^s/\partial \xi = Be^{-\xi/2}\cos((\eta+\pi)\beta)\sqrt{2\cosh\xi - 2\cos\eta}$$
$$\{(-e^{-\xi} + \cos\eta)(1-e^{-\xi\beta}) + 2\beta(\cosh\xi - \cos\eta)e^{-\xi\beta}\} \tag{5}$$

$$\partial T^\ell/\partial \eta = Ae^{-\xi/2}(e^{-\xi\beta} - 1)\sqrt{2\cosh\xi - 2\cos\eta}$$
$$\{2\beta(\cosh\xi - \cos\eta)(\kappa\sin(\eta\beta)\cos(\pi\beta) + \sin(\pi\beta)\cos(\eta\beta))$$
$$-\sin\eta(\kappa\cos(\eta\beta)\cos(\pi\beta) - \sin(\pi\beta)\sin(\eta\beta))\}/\cos(\eta\beta) \tag{6}$$

$$\partial T^\ell/\partial \xi = Ae^{-\xi/2}\{\kappa - \tan(\eta\beta)\tan(\pi\beta)\}\sqrt{2\cosh\xi - 2\cos\eta}$$
$$\cos(\beta\eta)\{(1-e^{-\xi\beta})(-e^{-\xi} + \cos\eta) + \beta(2\cosh\xi - 2\cos\eta)e^{-\xi\beta} \tag{7}$$

In eqns (3)-(7), A and B are constants to be determined by matching the two boundary element tangential gradients along the solid-liquid interface with those obtained by differentiating the asymptotic temperature distribution in the solid contact region. This asymptotic temperature is

$$T^s = T_0^s\{1 - \sqrt{2\cosh\xi - 2\cos\eta}e^{-\xi/2}(1-e^{-\xi\beta})\cos((\eta+\pi)\beta)\}, \tag{8}$$

where $\beta = \sqrt{\kappa/\varphi\pi}$ is a non-dimensional constant, and T_0^s is the numerically determined temperature in the middle of the dry spot.

4 Results

Figures 1-3 show the temperature distributions for a cell of H=h=R=5, with κ=0.1. Figure 1 shows the isothermal lines of a bubble with contact angle $\varphi=8^\circ$ and temperature T_f=0. The temperature distribution is symmetric about the cell axis and periodic at the edge of the cell. In the contact line region, the highly concentrated isothermal lines show an extremely high heat flux there, indicating that the major evaporation takes place in this region. Figure 2 shows that there is a condensation region on the top of the same bubble when T_f= -1. We omit most of the isothermal lines in the solid since they take almost the same pattern

as Fig. 1 and differ only in magnitude. Figure 3 enlarges the vicinity of the contact region, which is nearly of the same nature in all cases due to the Sadhal limit involved. For smaller κ, the temperature gradient should be steeper.

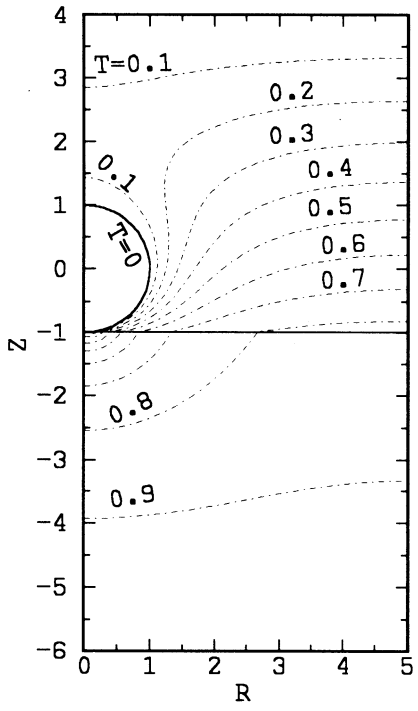


Figure 1
Isothermal lines with T_f=0

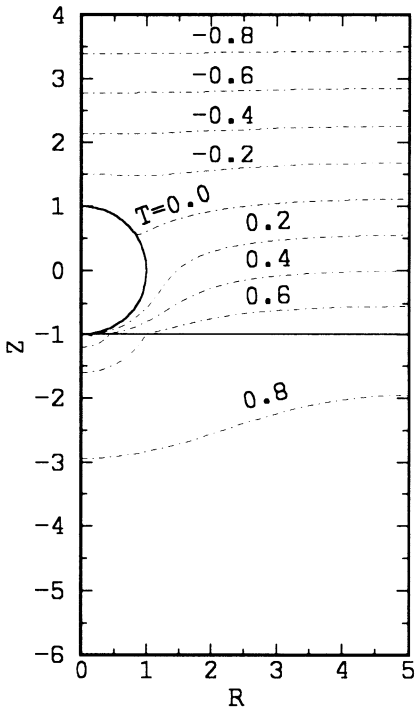


Figure 2
Isothermal lines with T_f=-1

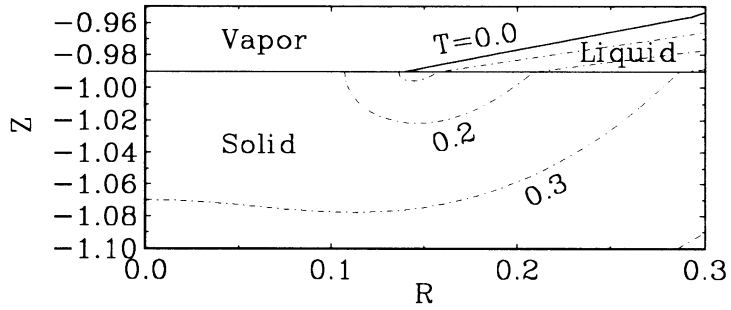


Figure 3
Isothermal lines in the vicinity of the contact region

Due to the large number of geometric and thermal parameters we focus our attention on several representative cases. When T_f=0, we define the parameters $\sigma_{s,\ell} = Q_s/Q_\ell$ and $\sigma_{v,s} = Q_v/Q_s$, where Q_s is the total heat supplied through the solid-liquid interface, Q_v as the total heat absorbed by the vapor bubble, and Q_ℓ as the total heat supplied through the solid-liquid interface in the absence of the bubble. $\sigma_{s,\ell}$ is the heat transfer enhancement due to the bubble's presence and $\sigma_{v,s}$ is the fraction of heat leaving the solid that contributes to vaporization.

To facilitate comparison when the bubble/cell ratio is big, all of the following calculations use the same ratio $\omega = (\bar{a} / R_c)^2$ of the bubble/cell areas, where $\bar{a}$ is the maximum horizontal half dimension of the bubble. Namely, if the bubble is suspended or attached but the contact angle of the attached bubble is less or equal to 90°, then $\bar{a}$ is the radius of the curvature of the bubble; if the bubble is attached and the contact angle is greater than 90°, then $\bar{a}$ is the radius of the dry spot. This definition is convenient for experiments since ω is simply the ratio of bubble/cell projection areas.

1) *The Influence of Bubble Position on Heat Transfer*: Figure 4 depicts the effect of bubble position on the heat enhancement $\sigma_{s,\ell}$ for zero liquid free surface temperature T_f. In Figure 4, R_c =H=h=5, and the results are plotted against $\delta = (d-1)/2$, where d is positive when the bubble is detached or when $\varphi < 90^\circ$; otherwise, it is negative. The resulting positive, zero and negative δ correspond to detached, tangential and attached bubbles respectively.

As parameters we take the ratio κ of the liquid to solid thermal conductivities and the different solid layer thicknesses λ=H/h=1, 5 and 10. There are a few aspects worth noticing. The first is that attached bubbles exhibit a far stronger solid coupling effect (i.e., greatly enhances heat transfer) than the detached ones, especially when κ is small. The second is when the bubble is attached, the heat transfer enhancement is, remarkably, neither sensitive to the various contact angle of the bubble (Figure 5) nor to the thickness of the solid layer. The third is that when the bubble is detached, the coupling effect of the solid on the heat transfer enhancement disappears quickly as the bubble leaves the solid-liquid interface. Finally, for poorly conducting liquids, the enhancement is most dramatic.

2) *The Influence of Bubble Density on the Heat Transfer*. Figure 5 shows the influence of bubble crowding by plotting the heat transfer enhancement ratio $\sigma_{s,\ell}$ as a function of the ratio ω of bubble to cell areas, with various parameters. The solid and liquid layer thicknesses are H=h=5, and T_f =0 for both κ = 0.01 and κ = 0.001. The bubble positions have three different contact angles φ = 30°, 90°, 150°. Of interest is the fact all curves converge to unity when the ω approaches zero, i.e., for large cells or tiny bubble, the overall enhanced heat flow in the whole cell induced by the existence of the bubble becomes insignificant. Inversely, the heat transfer increases rapidly when the cell size shrinks, i.e., when ω becomes order one, if the Sadhal limit is still valid

there. In Figure 5, this can be as much as 40 times that of large cells when κ = 0.01, or as large as 200 when κ = 0.001. This occurs because a large bubble alters the temperature distribution by forcing the isothermal lines to cross the solid-liquid interface in a much more bunched-up manner. This phenomenon can explain the sudden burst in the heat transfer rate associated with the incipience of nucleate pool boiling.

3) *The inhibition activity of an active nucleate site*: For various bubble positions and ratios of conductivities, Fig. 6 examines the fraction $\sigma_{v,s}$ of heat derived from the solid that goes towards liquid vaporization. Figure 6 shows that 95% of the total heat that passes through the solid-liquid interface finds its way to the liquid-vapor interface when the radius of the cell is smaller than 2.3, regardless of δ or κ. When the radius of cell is about 3 ($\omega \approx 0.11$), more than 80% of the heat passing through the solid-liquid interface enters the bubble, with only weak bubble position dependence. Obviously, the bubble acts as a major heat sink that monopolizes a considerable amount of the heat in its vicinity. As it grows, it alters the local temperature distribution leaving rather weak temperature gradients at a moderate distance from the bubble. This may be the cause of the observed inhibition activity [8]. Also the bubble frequency plays an important role in the process of altering the local temperature. Less frequent bubble emission at a site allows its neighboring sites to activate quickly; this can then reactivate the initial site. In contrast, frequent emission of one site does not allow neighboring sites to activate and thus inhibits the overall heat transfer.

5 Discussion

The quasi-steady analysis of heat transfer to a bubble from a solid wall in a finite composite cell can help explore the fundamental mechanism of nucleate boiling heat transfer. Our results demonstrate that heat conduction alone can contribute a tremendous amount to the overall heat transfer in nucleate boiling, especially when the bubble is attached. For attached bubbles, the solid-liquid coupling plays an important role in enhancing the heat transfer rate, while for detached bubbles such coupling effects disappear rapidly. In both cases, increasing bubble density strongly increases the overall heat transfer rate, as long as there is still a significant wetted area. The results also show that the enormous heat sink capability of a bubble alters the temperature profile in its vicinity and can deactivate neighboring sites.

Finally, it is important to note that unlike the unbounded solution of Sadhal (1989) and semi-infinite solution of Huang and Dagan (1993), the present results reveal several factors that can dramatically increase heat transfer by a few orders of magnitude. Most important is a higher solid-liquid conductivity ratio. Cases of lesser importance are the maintenance of very thin solid layers, and higher liquid temperatures, the latter of which is generally not practical. It is also very important to keep the bubbles on the solid-liquid interface, where

the heat transfer is the most effective, for as long as possible and also try to increase the bubble density (as long as there is still significant wetted area) by increasing the density of active nucleation sites.

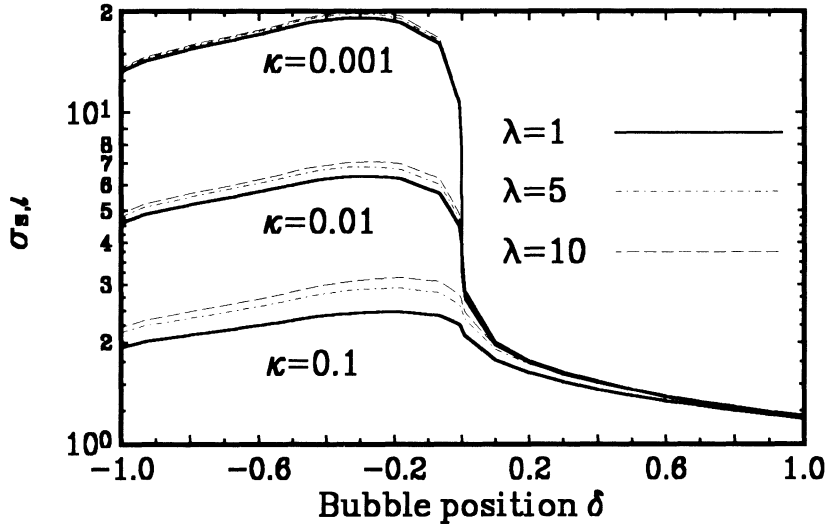


Figure 4
Heat transfer enhancement

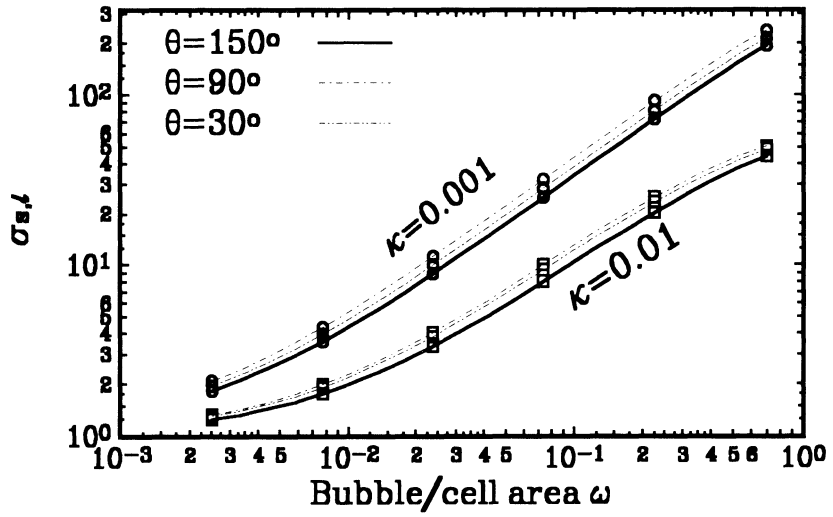


Figure 5
Heat transfer enhancement $\sigma_{s,l}$

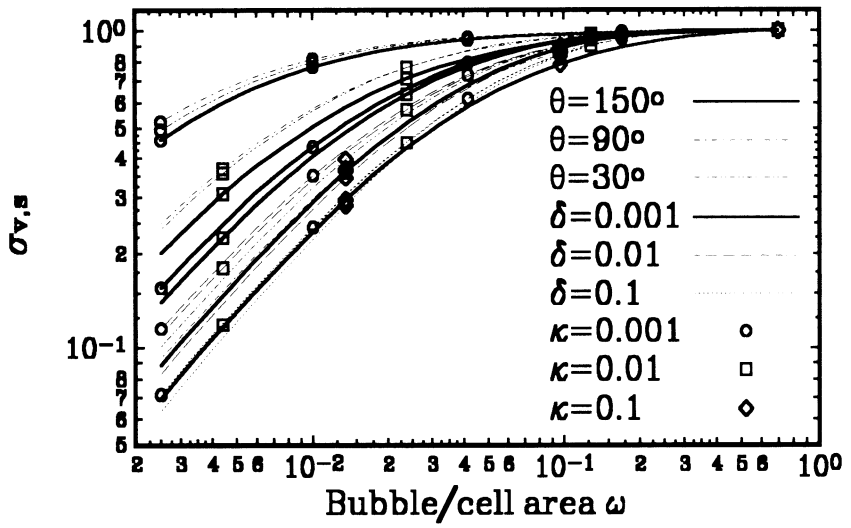


Figure 6
Vaporization factor $\sigma_{v,s}$

Reference

1. L.E. Scriven, On the dynamics of phase growth, *Chem. Engng Sci*, 1959, **10(1),** 1-14.
2. S.S.Sadhal, Heat transport to a slowly growing bubble on a solid surface, *Q Jl Mech. Appl. Math.*, 1989, **42**, Pt. 4, 477-493.
3. L.Huang, Z.Dagan, Heat transfer to a bubble suspended in a liquid layer near a solid plate, in *33rd Heat Transfer and Fluid Mechanics Institute*, (ed Frederick H. Reardon), pp. 211-233, California State University, Sacramento, June, 1993.
4. R.I.Eddington, D.B.R.Kenning and A.I.Korneichev, Comparison of gas and vapor bubble nucleation on a brass surface in water, *Int. J. Heat Transfer*, 1978, **21**, 855-862.
5. R.I.Eddington and D.B.R.Kenning, The prediction of low boiling bubble population from gas bubble nucleation experiments, *Proc. 6th Int. Heat Transfer Conference*, Toronto, Vol. 1, pp. 275-279, 1978.
6. R.L.Judd and C.H.Lavadas, The nature of nucleation site interaction, *J. Heat Transfer*, 1980, **102**, 461-464.
7. V.V.Chekanov, Interaction of centers in nucleate boiling, *Teplofiz, Vysok. Temp.*, 1977, **15**, 121-128.
8. A.Calka and R.L.Judd, Some aspects of the interaction among nucleation sites during saturated nucleate boiling, *Int. J. Heat Mass Transfer*, 1985, **28**, No.12, 2331-2342.